Do we really need the torus? Lessons learned from the humble slab

T. G. Adkins[1], P. G. Ivanov[1], D. Kennedy[2], M. Giacomin[3],
A. A. Schekochihin[1], and the Oxford Theory Group

[1]Rudolf Peierls Centre For Theoretical Physics,
University of Oxford,
Oxford, OX1 3PU, UK

[2]Culham Centre for Fusion Energy,
United Kingdom Atomic Energy Authority,
Abingdon, OX14 3EB, UK

[3]York Plasma Institute,
University of York,
York, YO10 5DD, UK

14th Plasma Kinetics Working Meeting, 26/07/23

Table of Contents

Table of Contents

Introduction

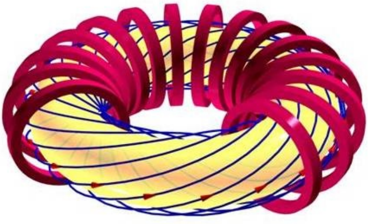

- Understanding (turbulent) heat transport in magnetically confined plasmas is crucial to the design of successful tokamak experiments

Introduction

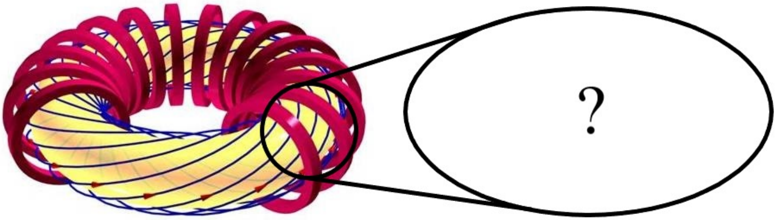

- Understanding (turbulent) heat transport in magnetically confined plasmas is crucial to the design of successful tokamak experiments
- These systems are incredibly **complicated**; what methods can we use to better understand them?

Introduction

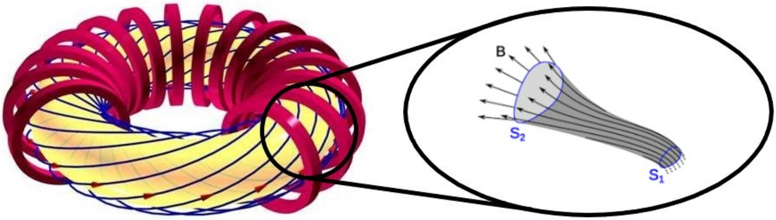

- Understanding (turbulent) heat transport in magnetically confined plasmas is crucial to the design of successful tokamak experiments
- These systems are incredibly **complicated**; what methods can we use to better understand them?

Introduction

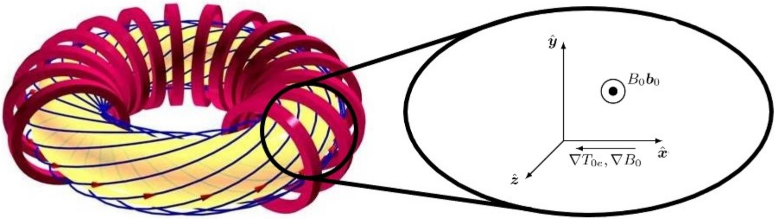

- Understanding (turbulent) heat transport in magnetically confined plasmas is crucial to the design of successful tokamak experiments
- These systems are incredibly **complicated**; what methods can we use to better understand them?
- Focus on two particular instances of where physics results derived in the context of reduced models carries over to the tokamak torus:
  i) **Scale invariance** of electrostatic drift-kinetics
  ii) The **thermo-Alfvénic instability** (TAI)

Table of Contents

Scale invariance

- Electrostatic ($\beta_s \to 0$) drift-kinetic ($k_\perp \rho_s \ll 1$) limit of gyrokinetics:

$$\frac{\partial}{\partial t}\left(h_s - \frac{q_s\phi}{T_{0s}} f_{0s}\right) + \left(v_\parallel \boldsymbol{b}_0 + \boldsymbol{v}_{ds}\right) \cdot \boldsymbol{\nabla} h_s + \frac{c}{B_0}\boldsymbol{b}_0 \cdot \left[\boldsymbol{\nabla}\phi \times \boldsymbol{\nabla}\left(h_s + f_{0s}\right)\right] = \sum_{s'} C^{(\ell)}_{ss'}[h_s],$$

$$0 = \sum_s q_s \left[-\frac{q_s\phi}{T_{0s}} n_{0s} + \int \mathrm{d}^3\boldsymbol{v}\, \langle h_s \rangle_{\boldsymbol{r}}\right].$$

Scale invariance

- Electrostatic ($\beta_s \to 0$) drift-kinetic ($k_\perp \rho_s \ll 1$) limit of gyrokinetics:

$$\frac{\partial}{\partial t}\left(h_s - \frac{q_s\phi}{T_{0s}} f_{0s}\right) + \left(v_\parallel \boldsymbol{b}_0 + \boldsymbol{v}_{ds}\right)\cdot \boldsymbol{\nabla} h_s + \frac{c}{B_0}\boldsymbol{b}_0 \cdot \left[\boldsymbol{\nabla}\phi \times \boldsymbol{\nabla}\left(h_s + f_{0s}\right)\right] = \sum_{s'} C^{(\ell)}_{ss'}[h_s],$$

$$0 = \sum_s q_s \left[-\frac{q_s\phi}{T_{0s}} n_{0s} + \int \mathrm{d}^3\boldsymbol{v}\,\langle h_s\rangle_{\boldsymbol{r}}\right].$$

- One-parameter transformation:

$$\tilde{h}_s^{\mathrm{even}} = \lambda^2\, h_s^{\mathrm{even}}(x/\lambda^2, y/\lambda^2, z/\lambda^{2/\alpha}, t/\lambda^2),$$
$$\tilde{h}_s^{\mathrm{odd}} = \lambda^{2/\alpha}\, h_s^{\mathrm{odd}}(x/\lambda^2, y/\lambda^2, z/\lambda^{2/\alpha}, t/\lambda^2),$$
$$\tilde{\phi} = \lambda^2\, \phi(x/\lambda^2, y/\lambda^2, z/\lambda^{2/\alpha}, t/\lambda^2),$$

for any λ. Note $\alpha = 1, 2$ in the collisionless ($\nu_* \to 0$) and collisional ($\nu_* \gg 1$) limits, respectively.

Scale invariance

- Electrostatic ($\beta_s \to 0$) drift-kinetic ($k_\perp \rho_s \ll 1$) limit of gyrokinetics:

$$\frac{\partial}{\partial t}\left(h_s - \frac{q_s\phi}{T_{0s}} f_{0s}\right) + \left(v_\parallel \boldsymbol{b}_0 + \boldsymbol{v}_{ds}\right)\cdot \boldsymbol{\nabla} h_s + \frac{c}{B_0}\boldsymbol{b}_0 \cdot \left[\boldsymbol{\nabla}\phi \times \boldsymbol{\nabla}\left(h_s + f_{0s}\right)\right] = \sum_{s'} C^{(\ell)}_{ss'}[h_s],$$

$$0 = \sum_s q_s \left[-\frac{q_s\phi}{T_{0s}} n_{0s} + \int \mathrm{d}^3\boldsymbol{v}\, \langle h_s \rangle_{\boldsymbol{r}}\right].$$

- One-parameter transformation:

$$\tilde{h}_s^{\mathrm{even}} = \lambda^2\, h_s^{\mathrm{even}}(x/\lambda^2, y/\lambda^2, z/\lambda^{2/\alpha}, t/\lambda^2),$$
$$\tilde{h}_s^{\mathrm{odd}} = \lambda^{2/\alpha}\, h_s^{\mathrm{odd}}(x/\lambda^2, y/\lambda^2, z/\lambda^{2/\alpha}, t/\lambda^2),$$
$$\tilde{\phi} = \lambda^2\, \phi(x/\lambda^2, y/\lambda^2, z/\lambda^{2/\alpha}, t/\lambda^2),$$

  for any λ. Note $\alpha = 1, 2$ in the collisionless ($\nu_* \to 0$) and collisional ($\nu_* \gg 1$) limits, respectively.

- Mathematically, the existence of this symmetry is a consequence of the **scale invariance** of electrostatic DK.

Implications for transport

- Suppose that our original solutions were periodic in x, y and z with domain sizes L_x, L_y and $L_\parallel$, respectively. Then, the transformed solutions will still be periodic in x, y and z, except now with domain sizes $\lambda^2 L_x$, $\lambda^2 L_y$ and $\lambda^{2/\alpha} L_\parallel$.

Implications for transport

- Suppose that our original solutions were periodic in x, y and z with domain sizes L_x, L_y and $L_\parallel$, respectively. Then, the transformed solutions will still be periodic in x, y and z, except now with domain sizes $\lambda^2 L_x$, $\lambda^2 L_y$ and $\lambda^{2/\alpha} L_\parallel$.
- Electrostatic heat flux

$$Q_s = n_{0s} T_{0s} \int \frac{\mathrm{d}^3\boldsymbol{r}}{V} \, (\boldsymbol{v}_E \cdot \boldsymbol{\nabla} x) \frac{\delta T_s}{T_{0s}},$$

will transform as:

$$\tilde{Q}_s(\lambda^2 L_x, \lambda^2 L_y, \lambda^{2/\alpha} L_\parallel, t/\lambda^2) = \lambda^2 Q_s(L_x, L_y, L_\parallel, t).$$

Implications for transport

- Suppose that our original solutions were periodic in x, y and z with domain sizes L_x, L_y and $L_\parallel$, respectively. Then, the transformed solutions will still be periodic in x, y and z, except now with domain sizes $\lambda^2 L_x$, $\lambda^2 L_y$ and $\lambda^{2/\alpha} L_\parallel$.
- Electrostatic heat flux

$$Q_s = n_{0s} T_{0s} \int \frac{\mathrm{d}^3 \boldsymbol{r}}{V} \, (\boldsymbol{v}_E \cdot \boldsymbol{\nabla} x) \frac{\delta T_s}{T_{0s}},$$

will transform as:

$$\tilde{Q}_s(\lambda^2 L_x, \lambda^2 L_y, \lambda^{2/\alpha} L_\parallel, t/\lambda^2) = \lambda^2 Q_s(L_x, L_y, L_\parallel, t).$$

- **Locality**: Q_s is independent of perpendicular domain size (local DK).

Implications for transport

- Suppose that our original solutions were periodic in x, y and z with domain sizes L_x, L_y and $L_\parallel$, respectively. Then, the transformed solutions will still be periodic in x, y and z, except now with domain sizes $\lambda^2 L_x$, $\lambda^2 L_y$ and $\lambda^{2/\alpha} L_\parallel$.
- Electrostatic heat flux

$$Q_s = n_{0s} T_{0s} \int \frac{\mathrm{d}^3\boldsymbol{r}}{V} \, (\boldsymbol{v}_E \cdot \boldsymbol{\nabla} x) \, \frac{\delta T_s}{T_{0s}},$$

will transform as:

$$\tilde{Q}_s(\lambda^2 L_x, \lambda^2 L_y, \lambda^{2/\alpha} L_\parallel, t/\lambda^2) = \lambda^2 Q_s(L_x, L_y, L_\parallel, t).$$

- **Locality**: Q_s is independent of perpendicular domain size (local DK).

Implications for transport

- Suppose that our original solutions were periodic in x, y and z with domain sizes L_x, L_y and $L_\parallel$, respectively. Then, the transformed solutions will still be periodic in x, y and z, except now with domain sizes $\lambda^2 L_x$, $\lambda^2 L_y$ and $\lambda^{2/\alpha} L_\parallel$.
- Electrostatic heat flux

  $$Q_s = n_{0s} T_{0s} \int \frac{\mathrm{d}^3 \boldsymbol{r}}{V} \, (\boldsymbol{v}_E \cdot \boldsymbol{\nabla} x) \frac{\delta T_s}{T_{0s}},$$

  will transform as:

  $$\tilde{Q}_s(\lambda^2 L_x, \lambda^2 L_y, \lambda^{2/\alpha} L_\parallel, t/\lambda^2) = \lambda^2 Q_s(L_x, L_y, L_\parallel, t).$$

- **Locality**: Q_s is independent of perpendicular domain size (local DK).
- **Stationarity**: Q_s has been able to reach a statistical steady-state.

Implications for transport

- Suppose that our original solutions were periodic in x, y and z with domain sizes L_x, L_y and $L_\parallel$, respectively. Then, the transformed solutions will still be periodic in x, y and z, except now with domain sizes $\lambda^2 L_x$, $\lambda^2 L_y$ and $\lambda^{2/\alpha} L_\parallel$.
- Electrostatic heat flux

$$Q_s = n_{0s} T_{0s} \int \frac{\mathrm{d}^3 \boldsymbol{r}}{V} \, (\boldsymbol{v}_E \cdot \boldsymbol{\nabla} x) \frac{\delta T_s}{T_{0s}},$$

will transform as:

$$\tilde{Q}_s(\lambda^2 L_x, \lambda^2 L_y, \lambda^{2/\alpha} L_\parallel, t/\lambda^2) = \lambda^2 Q_s(L_x, L_y, L_\parallel, t).$$

- **Locality**: Q_s is independent of perpendicular domain size (local DK).
- **Stationarity**: Q_s has been able to reach a statistical steady-state.

Implications for transport

- Suppose that our original solutions were periodic in x, y and z with domain sizes L_x, L_y and $L_\parallel$, respectively. Then, the transformed solutions will still be periodic in x, y and z, except now with domain sizes $\lambda^2 L_x$, $\lambda^2 L_y$ and $\lambda^{2/\alpha} L_\parallel$.
- Electrostatic heat flux

$$Q_s = n_{0s} T_{0s} \int \frac{\mathrm{d}^3\boldsymbol{r}}{V} \, (\boldsymbol{v}_E \cdot \boldsymbol{\nabla} x) \, \frac{\delta T_s}{T_{0s}},$$

will transform as:

$$\tilde{Q}_s(\lambda^2 L_x, \lambda^2 L_y, \lambda^{2/\alpha} L_\parallel, t/\lambda^2) = \lambda^2 Q_s(L_x, L_y, L_\parallel, t).$$

- **Locality**: Q_s is independent of perpendicular domain size (local DK).
- **Stationarity**: Q_s has been able to reach a statistical steady-state.
- Given that λ can be chosen arbitrarily, it follows that:

$$\boxed{Q_s \propto L_\parallel^\alpha}$$

Scale invariance in a slab

$$\frac{\partial}{\partial t}\bar{\tau}^{-1}\varphi - \frac{c_1 v_{\mathrm{the}}^2}{2\nu_{ei}}\frac{\partial^2}{\partial z^2}\left[\left(1+\frac{1}{\bar{\tau}}\right)\varphi - \left(1+\frac{c_2}{c_1}\right)\frac{\delta T_e}{T_{0e}}\right] = 0,$$

$$\frac{\mathrm{d}}{\mathrm{d}t}\frac{\delta T_e}{T_{0e}} + \frac{2}{3}\frac{c_1 v_{\mathrm{the}}^2}{2\nu_{ei}}\frac{\partial^2}{\partial z^2}\left\{\left(1+\frac{1}{\bar{\tau}}\right)\left(1+\frac{c_2}{c_1}\right)\varphi - \left[\frac{c_3}{c_1} + \left(1+\frac{c_2}{c_1}\right)^2\right]\frac{\delta T_e}{T_{0e}}\right\}$$

$$= -\frac{\rho_e v_{\mathrm{the}}}{2L_T}\frac{\partial \varphi}{\partial y}.$$

- Describes physics on scales:

$$k_\parallel L_T \sim \sqrt{\sigma}, \quad k_\perp \rho_\perp \sim 1, \quad \rho_\perp = \frac{\rho_e}{\sigma}\frac{L_T}{\lambda_{ei}},$$

where σ is some arbitrary constant satisfying

$$\underbrace{\beta_e}_{\text{EM effects}} \ll \sigma \ll \underbrace{1}_{\text{thermal diffusion}} .$$

- Manifestly **invariant** under the derived DK symmetry:

$$\delta\tilde{T}_e = \lambda^2 \delta T_e(x/\lambda^2, y/\lambda^2, z/\lambda, t/\lambda^2), \quad \tilde{\phi} = \lambda^2 \phi(x/\lambda^2, y/\lambda^2, z/\lambda, t/\lambda^2).$$

Scale invariance in a slab

$$\frac{\partial}{\partial t}\bar{\tau}^{-1}\varphi - \frac{c_1 v_{\mathrm{the}}^2}{2\nu_{ei}}\frac{\partial^2}{\partial z^2}\left[\left(1+\frac{1}{\bar{\tau}}\right)\varphi - \left(1+\frac{c_2}{c_1}\right)\frac{\delta T_e}{T_{0e}}\right] = 0,$$

$$\frac{\mathrm{d}}{\mathrm{d}t}\frac{\delta T_e}{T_{0e}} + \frac{2}{3}\frac{c_1 v_{\mathrm{the}}^2}{2\nu_{ei}}\frac{\partial^2}{\partial z^2}\left\{\left(1+\frac{1}{\bar{\tau}}\right)\left(1+\frac{c_2}{c_1}\right)\varphi - \left[\frac{c_3}{c_1} + \left(1+\frac{c_2}{c_1}\right)^2\right]\frac{\delta T_e}{T_{0e}}\right\}$$

$$= -\frac{\rho_e v_{\mathrm{the}}}{2L_T}\frac{\partial\varphi}{\partial y}.$$

- Characteristic parallel and perpendicular frequencies:

$$\omega_\parallel = c_1\frac{\left(k_\parallel v_{\mathrm{the}}\right)^2}{2\nu_{ei}}, \quad \omega_{*e} = \frac{k_y\rho_e v_{\mathrm{the}}}{2L_T}.$$

Scale invariance in a slab

$$\frac{\partial}{\partial t}\bar{\tau}^{-1}\varphi - \frac{c_1 v_{\mathrm{the}}^2}{2\nu_{ei}}\frac{\partial^2}{\partial z^2}\left[\left(1+\frac{1}{\bar{\tau}}\right)\varphi - \left(1+\frac{c_2}{c_1}\right)\frac{\delta T_e}{T_{0e}}\right] = 0,$$

$$\frac{\mathrm{d}}{\mathrm{d}t}\frac{\delta T_e}{T_{0e}} + \frac{2}{3}\frac{c_1 v_{\mathrm{the}}^2}{2\nu_{ei}}\frac{\partial^2}{\partial z^2}\left\{\left(1+\frac{1}{\bar{\tau}}\right)\left(1+\frac{c_2}{c_1}\right)\varphi - \left[\frac{c_3}{c_1} + \left(1+\frac{c_2}{c_1}\right)^2\right]\frac{\delta T_e}{T_{0e}}\right\}$$
$$= -\frac{\rho_e v_{\mathrm{the}}}{2L_T}\frac{\partial \varphi}{\partial y}.$$

- Characteristic parallel and perpendicular frequencies:

$$\omega_\parallel = c_1 \frac{\left(k_\parallel v_{\mathrm{the}}\right)^2}{2\nu_{ei}}, \quad \omega_{*e} = \frac{k_y \rho_e v_{\mathrm{the}}}{2L_T}.$$

- Supports the collisional slab ETG (sETG) instability (Adkins et al., 2022): for $\omega_\parallel \ll \omega \ll \omega_{*e}$,

$$\omega = \pm\frac{1 + i\,\mathrm{sgn}(k_y)}{\sqrt{2}}\left(1+\frac{c_2}{c_1}\right)^{1/2}\left(\omega_\parallel |\omega_{*e}| \bar{\tau}\right)^{1/2}.$$

Scale invariance in a slab

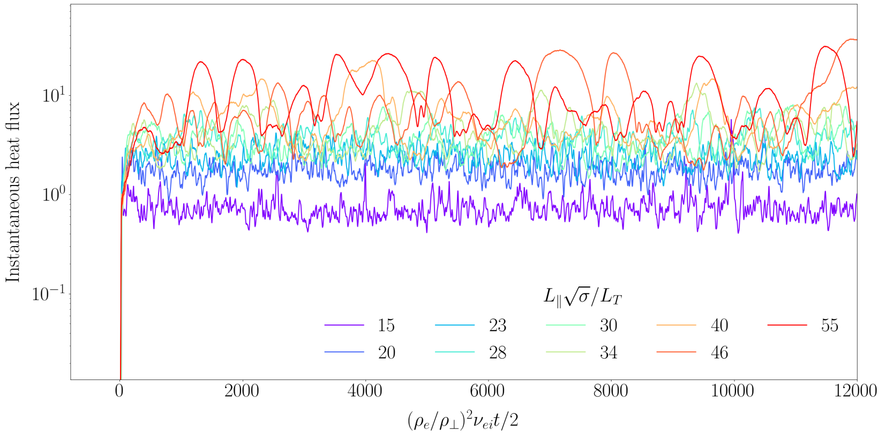

- We conducted a series of simulations in which we varied the parallel system size at fixed parallel resolution.
- Perpendicular hyperviscosity was introduced in order to provide an ultraviolet cutoff for the sETG instability. **Breaks scale invariance?**

Scale invariance in a slab

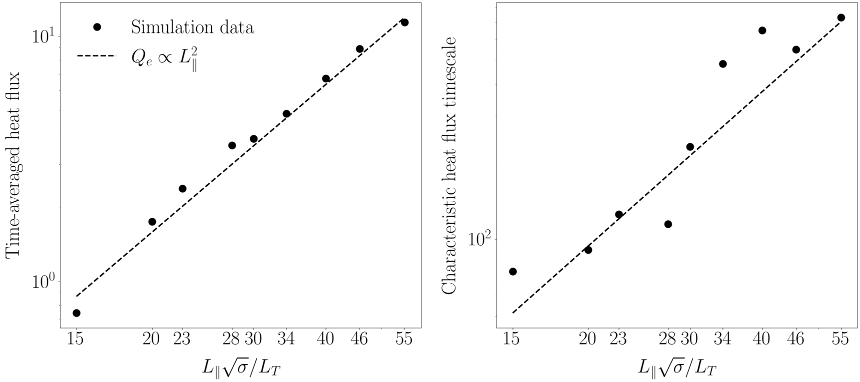

- Logarithmic fits to the data give slopes of 2.02 and 2.06, respectively.
- Appears to agree quite well with the predicted scaling. **But are the plasma dynamics?** See Adkins et al. (2023)

Scale invariance in a slab

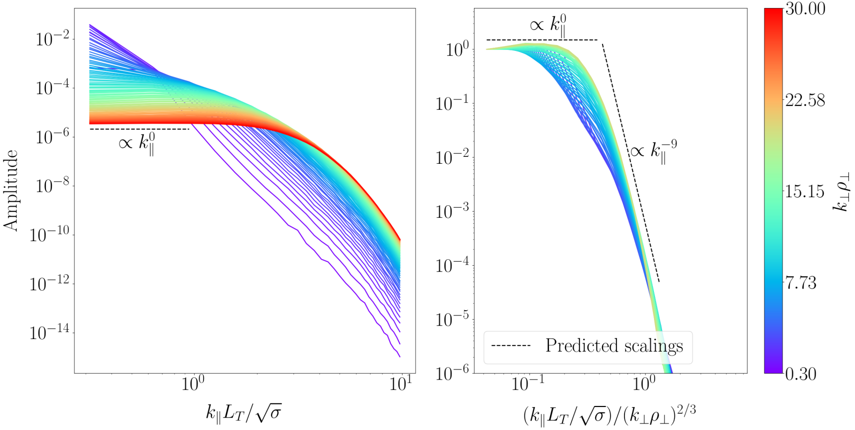

- Logarithmic fits to the data give slopes of 2.02 and 2.06, respectively.
- Appears to agree quite well with the predicted scaling. **But are the plasma dynamics?** See Adkins et al. (2023)

Scale invariance in a tokamak

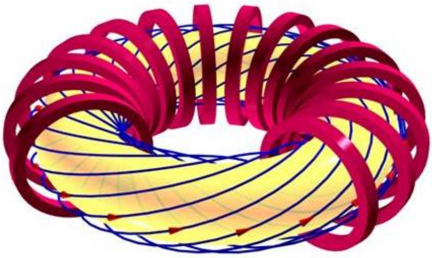

- So how do we extend these ideas to toroidal geometry?

Scale invariance in a tokamak

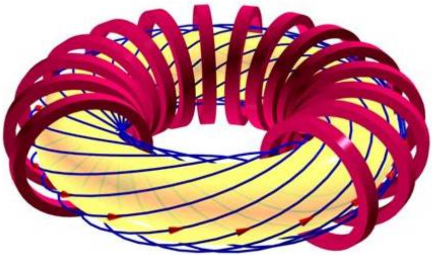

- So how do we extend these ideas to toroidal geometry?
- Scale invariance is broken by the existence of some spatial **inhomogeneity** of the (parallel) magnetic equilibrium. For a tokamak:

$$L_{\parallel} \sim \pi q R \quad \Rightarrow \quad Q_s \propto q^{\alpha}$$

Scale invariance in a tokamak

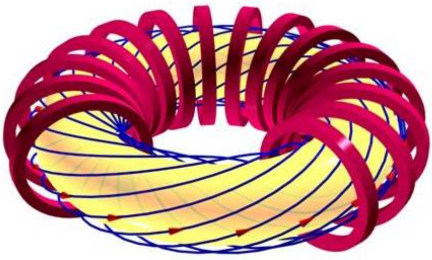

- So how do we extend these ideas to toroidal geometry?
- Scale invariance is broken by the existence of some spatial **inhomogeneity** of the (parallel) magnetic equilibrium. For a tokamak:

$$L_{\parallel} \sim \pi q R \quad \Rightarrow \quad Q_s \propto q^{\alpha}$$

- This could have implications for plasma systems in which magnetic fields have (significant) parallel structure on scales much shorter than the connection length e.g., edge plasmas (Parisi et al., 2020, 2022) or in stellerators (Roberg-Clark et al., 2022).

Scale invariance in a tokamak

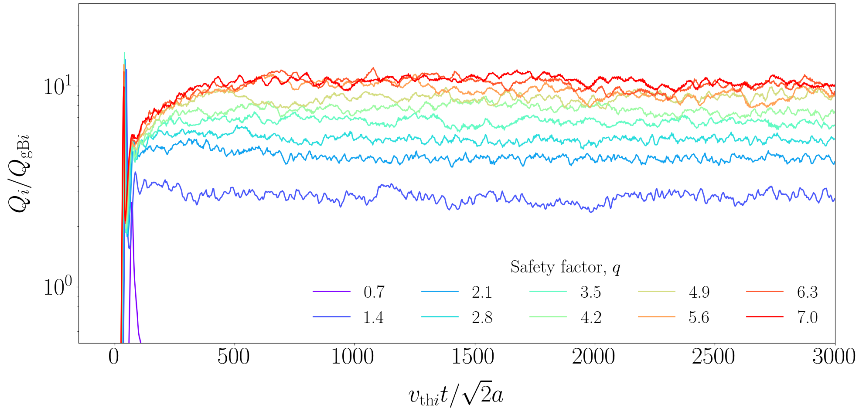

- We performed a series of ion-scale (adiabatic electron) simulations using the gyrokinetic code `GX` for Cyclone-Base-Case parameters (Dimits et al., 2000).
- Parameters: $r/a = 0.5$, $R/a = 2.8$, $\hat{s} = 0.8$, $a/L_{T_i} = 2.5$, $a/L_n = 0.8$, $\nu_{ii}/(v_{\mathrm{th}i}/a) = 1.2 \times 10^{-4}$.

Scale invariance in a tokamak

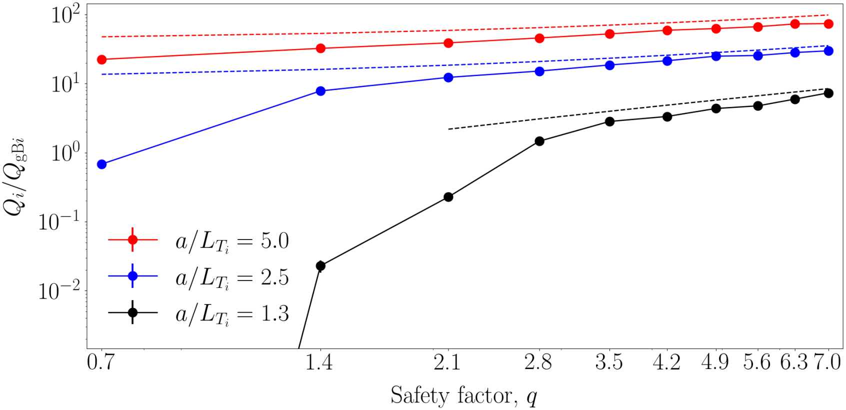

- Drop-off in transport at lower values of q appears to be consistent with the onset of the Dimits shift (see, e.g., Rogers et al., 2000).

Table of Contents

Instabilities above the d_e scale

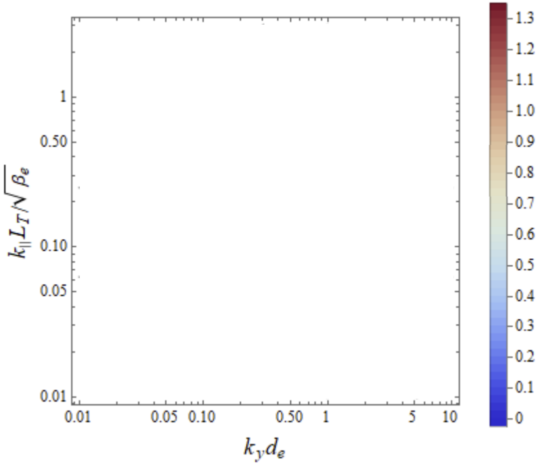

- The electron inertial scale $d_e = \rho_e/\sqrt{\beta_e}$ plays a key role in the linear (and nonlinear) dynamics of low-beta plasmas $\Rightarrow$ **flux-freezing scale**

Instabilities above the d_e scale

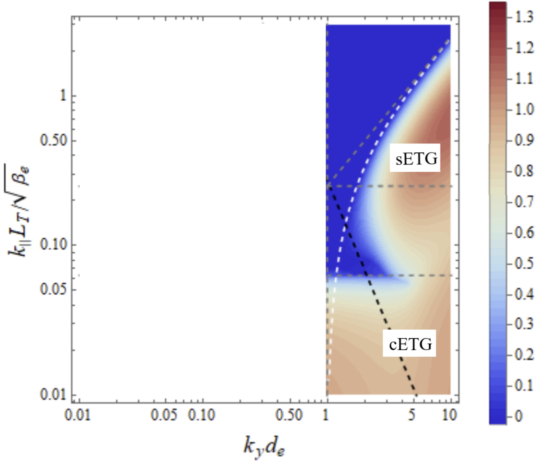

- At $k_\perp d_e \gg 1$, electrons are allowed to stream freely across unperturbed field lines. **sETG** and **cETG**, $\boldsymbol{E} \times \boldsymbol{B}$ drive.

Instabilities above the d_e scale

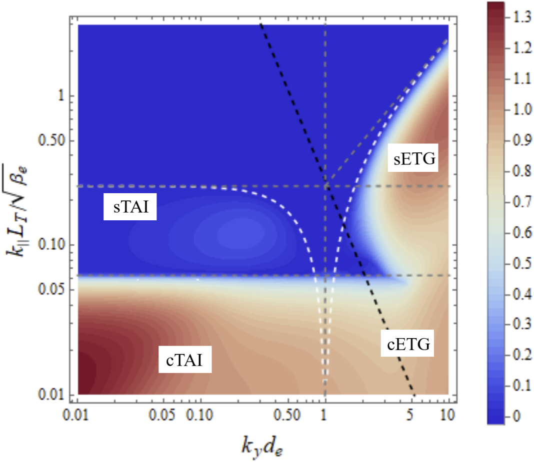

- At $k_\perp d_e \ll 1$, $\delta \boldsymbol{B}_\perp$ is created as electrons move along field lines and drag them along. **sTAI** and **cTAI**, magnetic flutter drive (as well as $\boldsymbol{E} \times \boldsymbol{B}$).

Curvature-mediated TAI

$$\frac{\mathrm{d}}{\mathrm{d}t}\frac{\delta n_e}{n_{0e}} = -\frac{\rho_e v_{\mathrm{the}}}{L_B}\frac{\partial}{\partial y}\frac{\delta T_e}{T_{0e}}, \quad \frac{\mathrm{d}\mathcal{A}}{\mathrm{d}t} + \frac{v_{\mathrm{the}}}{2}\frac{\partial \varphi}{\partial z} = \frac{v_{\mathrm{the}}}{2}\boldsymbol{\nabla}_\parallel \frac{\delta n_e}{n_{0e}}, \quad \underbrace{\boldsymbol{\nabla}_\parallel \frac{\delta T_e}{T_{0e}} = \frac{\rho_e}{L_T}\frac{\partial \mathcal{A}}{\partial y}}_{①},$$

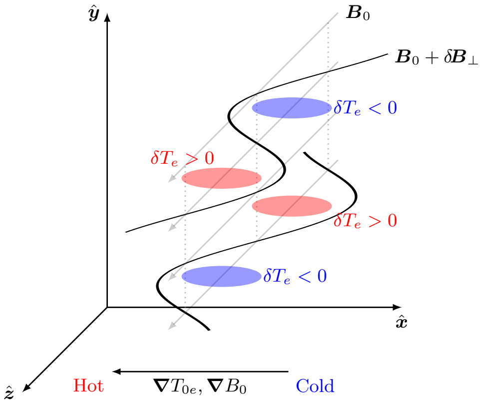

- A perturbation $\delta B_x = B_0 \rho_e \partial_y \mathcal{A}$ sets up a variation of total temp. along the perturbed field line as it makes excursions into hot and cold regions.
- Rapid thermal conduction along field lines creates a temperature perturbation that compensates for this.

Curvature-mediated TAI

$$\underbrace{\frac{\mathrm{d}}{\mathrm{d}t}\frac{\delta n_e}{n_{0e}} = -\frac{\rho_e v_{\mathrm{the}}}{L_B}\frac{\partial}{\partial y}\frac{\delta T_e}{T_{0e}}}_{②}, \quad \frac{\mathrm{d}\mathcal{A}}{\mathrm{d}t} + \frac{v_{\mathrm{the}}}{2}\frac{\partial \varphi}{\partial z} = \frac{v_{\mathrm{the}}}{2}\boldsymbol{\nabla}_{\parallel}\frac{\delta n_e}{n_{0e}}, \quad \boldsymbol{\nabla}_{\parallel}\frac{\delta T_e}{T_{0e}} = \frac{\rho_e}{L_T}\frac{\partial \mathcal{A}}{\partial y},$$

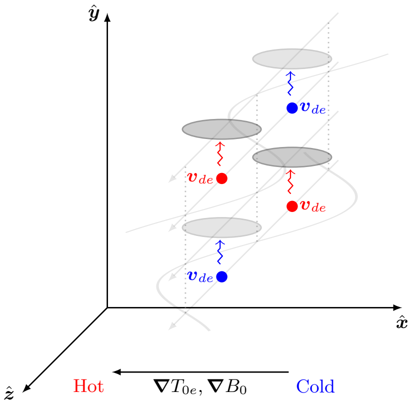

- Velocity dependence of magnetic drifts $\boldsymbol{v}_{de}$ creates an electron density perturbation (hot particles drift faster than cold ones).
- This electron density perturbation has both $k_y \neq 0$ and $k_{\parallel} \neq 0$.

Curvature-mediated TAI

$$\frac{\mathrm{d}}{\mathrm{d}t}\frac{\delta n_e}{n_{0e}} = -\frac{\rho_e v_{\mathrm{the}}}{L_B}\frac{\partial}{\partial y}\frac{\delta T_e}{T_{0e}}, \quad \underbrace{\frac{\mathrm{d}\mathcal{A}}{\mathrm{d}t} + \frac{v_{\mathrm{the}}}{2}\frac{\partial \varphi}{\partial z} = \frac{v_{\mathrm{the}}}{2}\boldsymbol{\nabla}_{\parallel}\frac{\delta n_e}{n_{0e}}}_{③}, \quad \boldsymbol{\nabla}_{\parallel}\frac{\delta T_e}{T_{0e}} = \frac{\rho_e}{L_T}\frac{\partial \mathcal{A}}{\partial y},$$

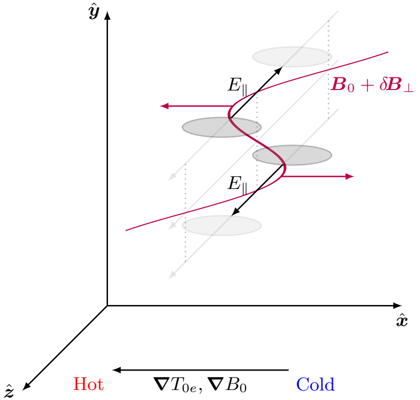

- The parallel density gradient must be balanced by the parallel electric field.
- Inductive part leads to an increase in δB_x, deforming the field line further into the hot and cold regions $\Rightarrow$ feedback.
- The does not require the usual $\boldsymbol{E} \times \boldsymbol{B}$ feedback mechanism to be present.

General TAI dispersion relation

- More generally, both the sTAI and cTAI can be captured in a single dispersion relation:

$$\boxed{\omega^2 = -\left(2\omega_{de}\omega_{*e} - \omega_{\mathrm{KAW}}^2\right)\left(\bar{\tau} + \frac{1}{1 + i\xi_*}\right),} \quad \xi_* = \frac{\sqrt{\pi}}{2}\frac{\omega_{*e}}{|k_\parallel| v_{\mathrm{the}}}.$$

- Also valid in the collisional regime, in which thermal conduction replaces parallel streaming as the relevant parallel timescale:

$$\xi_* = \frac{\sqrt{\pi}}{2}\frac{\omega_{*e}}{|k_\parallel| v_{\mathrm{the}}} \quad \Rightarrow \quad \xi_* = \frac{\omega_{*e}}{\kappa k_\parallel^2}.$$

- The general physical mechanism is the competition between the diamagnetic drifts (arising from the presence of the ETG) and rapid parallel streaming (collisionless) or thermal conduction (collisional) along perturbed magnetic field lines ⇒ accessing the magnetic flutter drive.

TAI in gyrokinetics

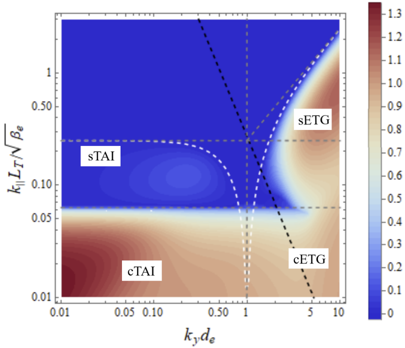

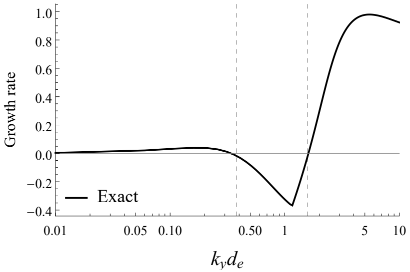

- Extensive details of the **Thermo-Alfvénic instability** can be found in Adkins et al. (2022).

TAI in gyrokinetics

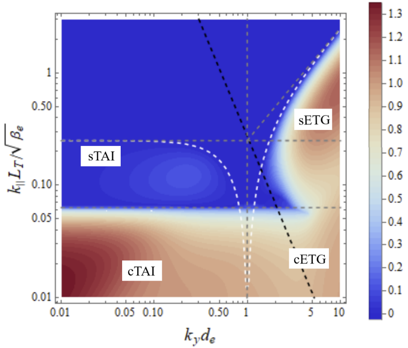

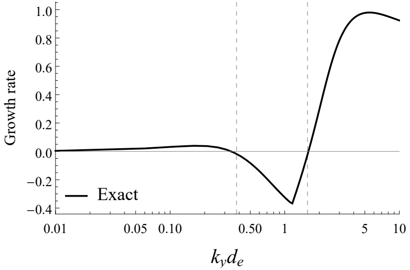

- Extensive details of the **Thermo-Alfvénic instability** can be found in Adkins et al. (2022).
- Can we recover the TAI in gyrokinetics? Following results from D. Kennedy (CCFE) and M. Giacomin (York)

TAI in gyrokinetics

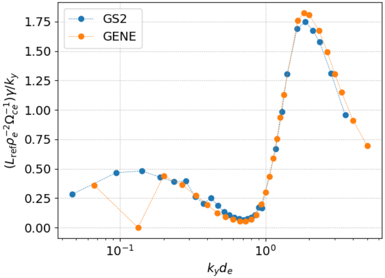

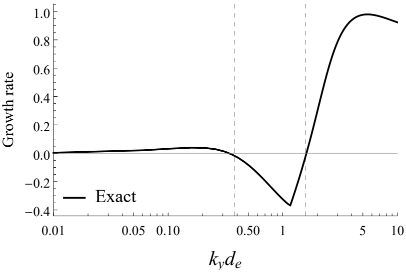

- Extensive details of the **Thermo-Alfvénic instability** can be found in Adkins et al. (2022).
- Can we recover the TAI in gyrokinetics? Following results from D. Kennedy (CCFE) and M. Giacomin (York)
- Performed simulations of sTAI in `GS2` and `GENE`, showing remarkably agreement with theory. Here, $L_{\mathrm{ref}}/L_{T_e} = 105$, $k_{\|,\mathrm{min}} = 0.03 L_T/\sqrt{\beta_e}$.

TAI in gyrokinetics

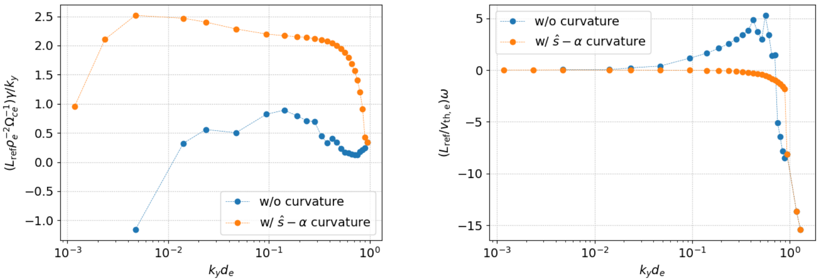

- What about **curvature**? Both `GS2` and `GENE` are also able to recover the cTAI in constant-curvature geometries.

TAI in gyrokinetics

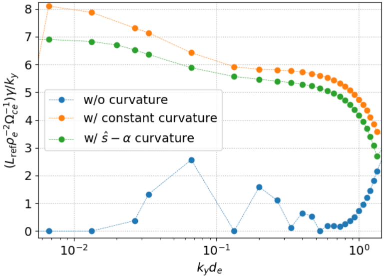

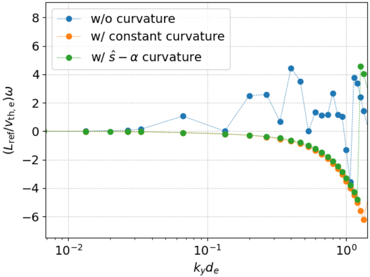

- What about **curvature**? Both `GS2` and `GENE` are also able to recover the cTAI in constant-curvature geometries.

TAI in gyrokinetics

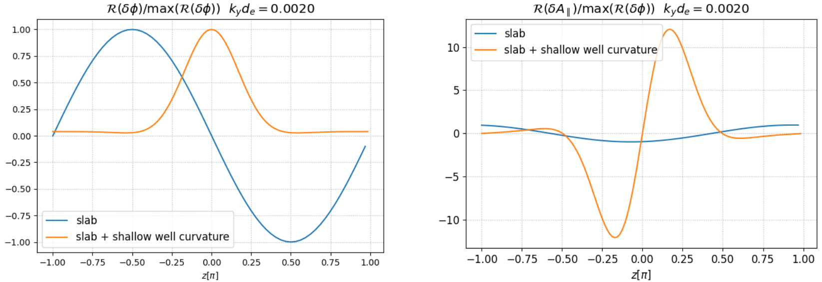

- What about **curvature**? Both `GS2` and `GENE` are also able to recover the cTAI in constant-curvature geometries.
- The sTAI and cTAI have different parity eigenfunctions, as expected. Both instabilities are **highly electromagnetic** in nature, with $\mathcal{A} \gg \varphi$.

TAI in gyrokinetics

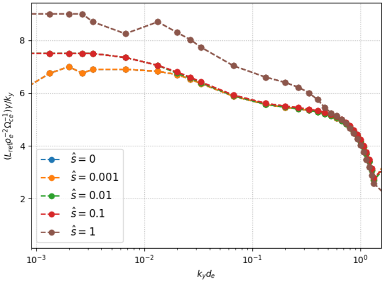

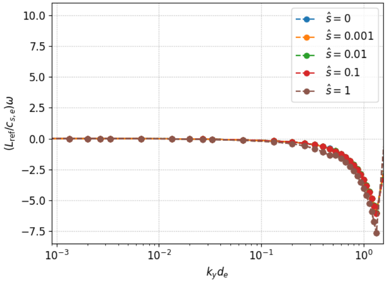

- Increase **complexity** further: **magnetic shear** + **Shafranov shift.**

TAI in gyrokinetics

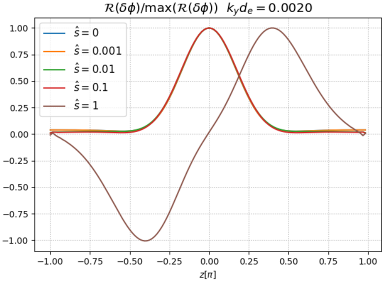

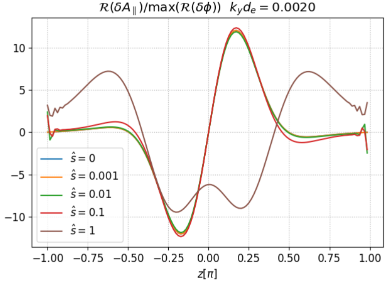

- Increase **complexity** further: **magnetic shear** + Shafranov shift.

TAI in gyrokinetics

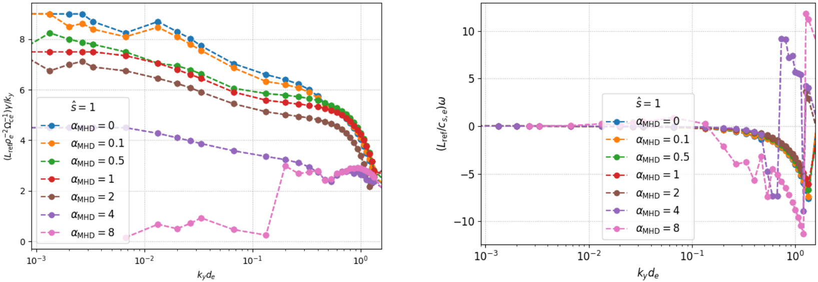

- Increase **complexity** further: magnetic shear + **Shafranov shift.**

TAI in gyrokinetics

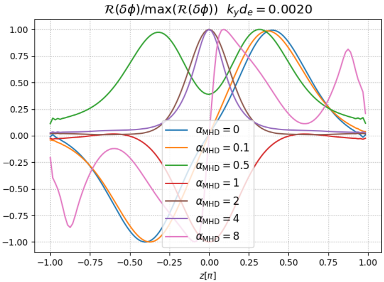

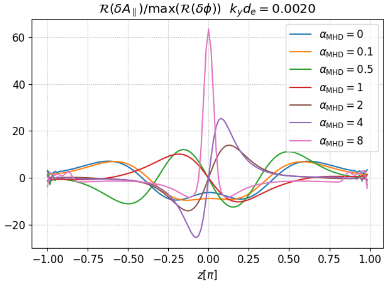

- Increase **complexity** further: magnetic shear + **Shafranov shift.**

TAI in gyrokinetics

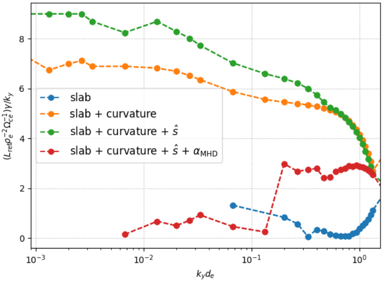

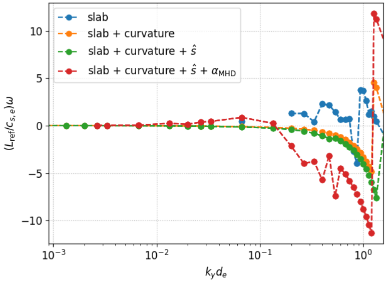

- Increase **complexity** further: **magnetic shear + Shafranov shift.**

TAI in gyrokinetics

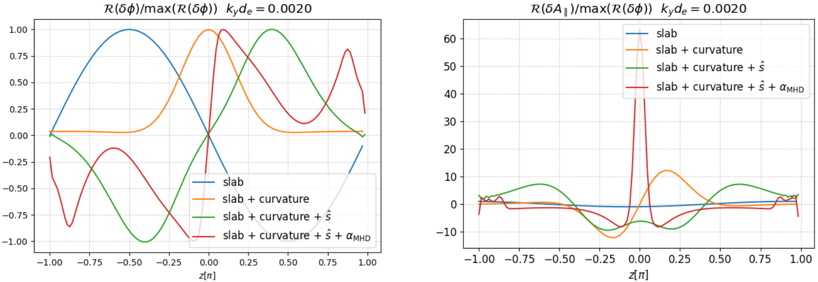

- Increase **complexity** further: **magnetic shear + Shafranov shift.**

TAI in gyrokinetics

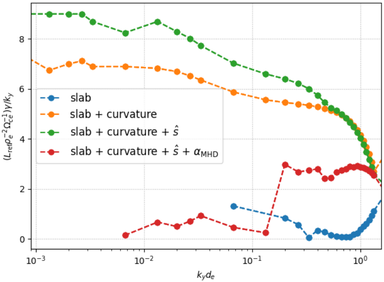

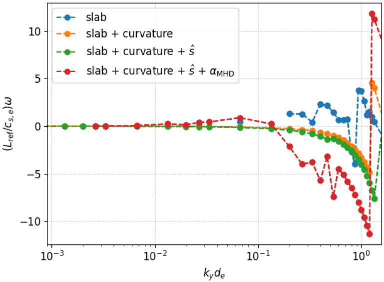

- Increase **complexity** further: **magnetic shear + Shafranov shift.**
- It appears that the TAI instability mechanism appears to survive the transition to toroidicity. **Another win for the slab?**

TAI in gyrokinetics

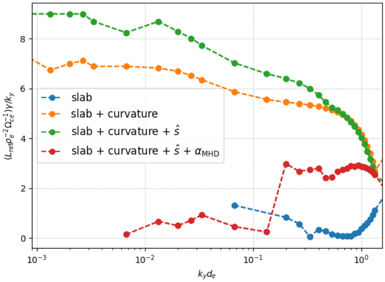

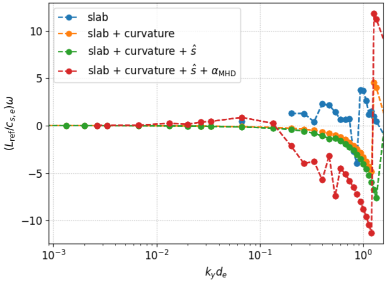

- Increase complexity further: **magnetic shear + Shafranov shift.**
- It appears that the TAI instability mechanism appears to survive the transition to toroidicity. **Another win for the slab?**
- We plan to further push towards a realistic (STEP relevant) tokamak geometry, and determine how TAI fits within the established electromagnetic instability "zoo".

Table of Contents

Electromagnetic sTAI-driven turbulence

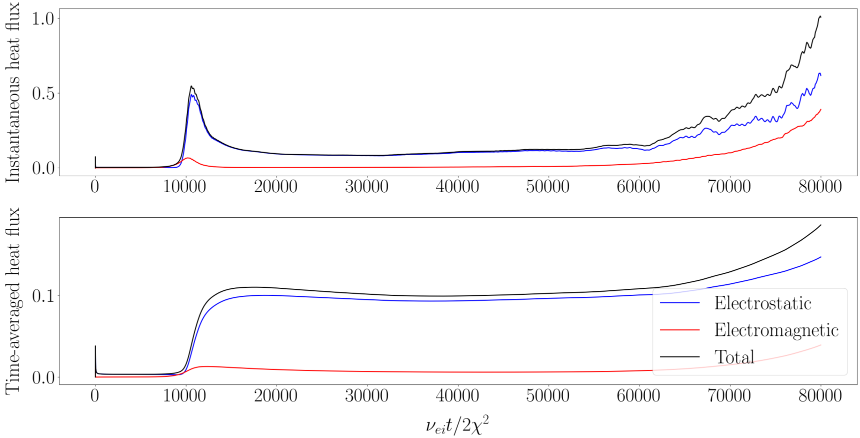

- Simulations of turbulence driven by the (collisional) sTAI display a lack of saturation similar to that seen in gyrokinetic codes.

Electromagnetic sTAI-driven turbulence

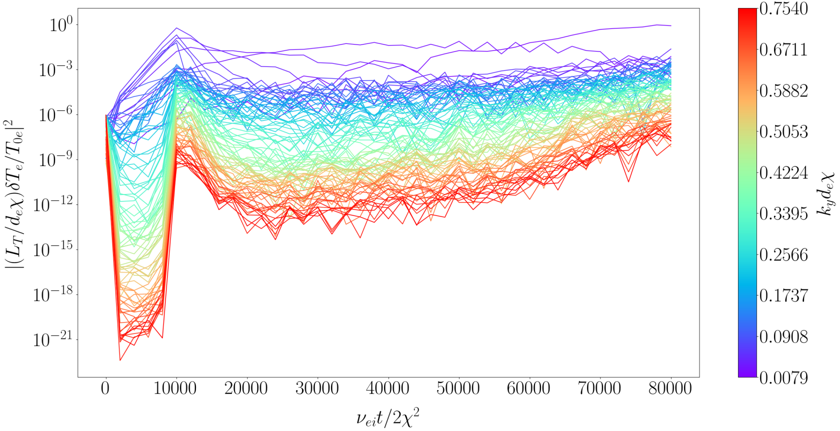

- The time-evolution of individual poloidal wavenumbers $k_y d_e \chi$ of the temperature perturbations. The dominant (growing) wavenumber at late times is $k_y d_e \chi = 0.0157$, corresponding to the second poloidal harmonic.

Electromagnetic sTAI-driven turbulence

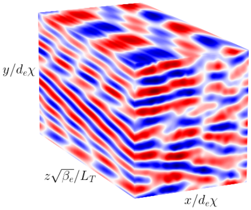

(a) $(L_T/d_e\chi)\varphi$

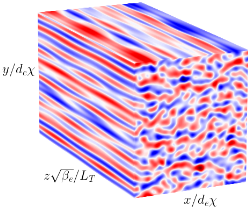

(b) $(L_T/d_e\chi)\delta T_e/T_{0e}$

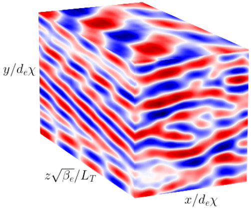

(c) $(L_T/d_e\chi^2)\mathcal{A}$

- The three-dimensional nature of the sTAI can be seen in the parallel structure manifest in all of the fields, as can the Alfvénic character of the instability in the fact that the electrostatic and magnetic vector potential perturbations are approximately in phase.

Electromagnetic sTAI-driven turbulence

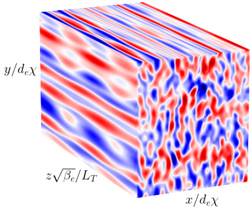

(a) $(L_T/d_e\chi)\varphi$

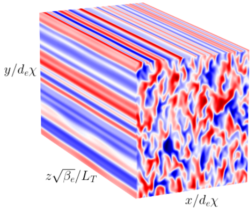

(b) $(L_T/d_e\chi)\delta T_e/T_{0e}$

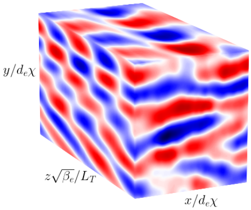

(c) $(L_T/d_e\chi^2)\mathcal{A}$

- The magnetic vector potential is now at significantly larger scales than the other two fields, displaying a streamer-like structure, albeit one with a non-zero $k_\parallel$.

Electromagnetic sTAI-driven turbulence

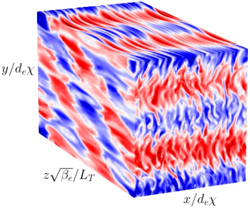

(a) $(L_T/d_e\chi)\varphi$

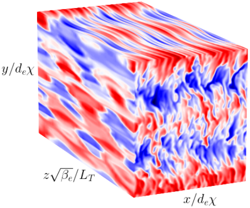

(b) $(L_T/d_e\chi)\delta T_e/T_{0e}$

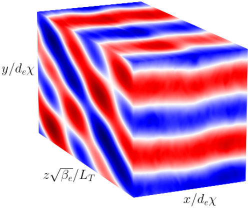

(c) $(L_T/d_e\chi^2)\mathcal{A}$

- The lack of saturation is associated with a now fully-developed streamer-like structure (with non-zero parallel and poloidal variation) in the parallel magnetic vector potential. This structure appears to be impervious to all mechanisms of nonlinear shearing.

Electromagnetic sTAI-driven turbulence

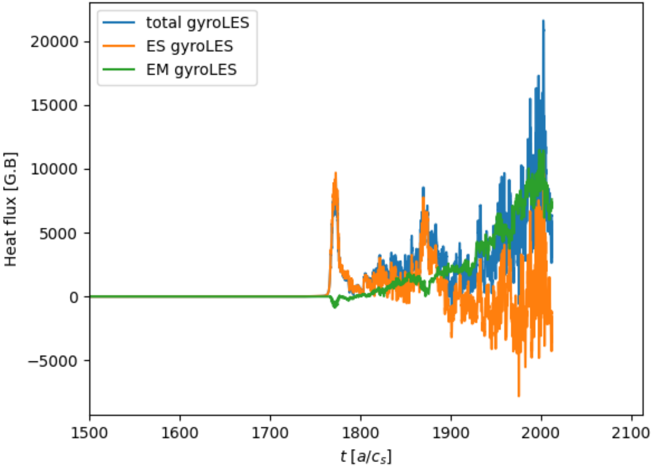

- This behaviour is reproduced in gyrokinetic simulations of sTAI turbulence

Electromagnetic sTAI-driven turbulence

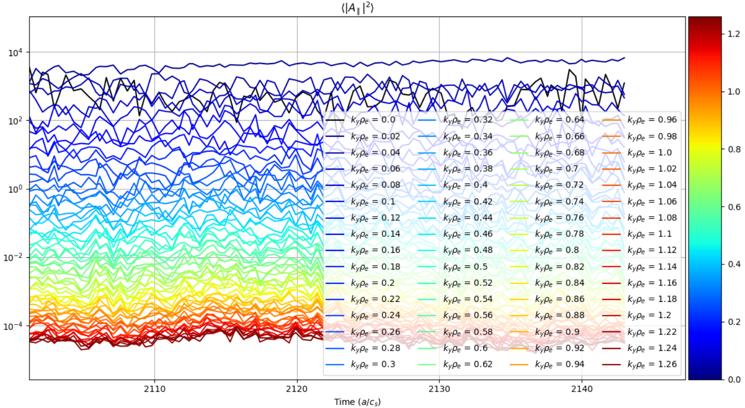

- This behaviour is reproduced in gyrokinetic simulations of sTAI turbulence ⇒ **minimal model that reproduces the gyrokinetic electromagnetic blow up.**

Table of Contents

Summary and future work

- **Scale invariance of gyrokinetic turbulence**.

SYMMETRY (scale invariance vs. $L_\parallel$)	$\Rightarrow$	**TRANSPORT** (heat flux scaling $Q_s \propto L_\parallel^\alpha$)

  Future work: extensions to more general geometries (stellarators), electromagnetic scale invariance (or not?)

- **The thermo-Alfvénic instability (TAI)** extracts free energy from the equilibrium temperature gradient through finite perturbations to the magnetic-field direction. Appears to survive the transition to toroidicity.

$$\boxed{\omega^2 = -\left(2\omega_{de}\omega_{*e} - \omega_{\mathrm{KAW}}^2\right)\left(\bar{\tau} + \frac{1}{1 + i\xi_*}\right),}$$

  Future work: probing the robustness of this survival (e.g., ions)

- **Electromagnetic "blow-ups"** reminiscent of those in full gyrokinetics appear to be reproducible in sTAI-driven turbulence. Future work: determining how (and whether) these blow-ups can be arrested in these simple models, application to more general gyrokinetic simulations.

Adkins, T., Ivanov, P. G. & Schekochihin, A. A. 2023 Scale invariance and critical balance in electrostatic drift-kinetic turbulence. *J. Plasma Phys.* **89**, 905890406.

Adkins, T., Schekochihin, A. A., Ivanov, P. G. & Roach, C. M. 2022 Electromagnetic instabilities and plasma turbulence driven by electron-temperature gradient. *J. Plasma Phys.* **88**, 905880410.

Dimits, A. M., Bateman, G., Beer, M. A., Cohen, B. I., Dorland, W., Hammett, G. W., Kim, C., Kinsey, J. E., Kotschenreuther, M., Kritz, A. H., Lao, L. L., Mandrekas, J., Nevins, W. M., Parker, S. E., Redd, A. J., Shumaker, D. E., Sydora, R. & Weiland, J. 2000 Comparisons and physics basis of tokamak transport models and turbulence simulations. *Phys. Plasmas* **7**, 969.

Parisi, J. F., Parra, F. I., Roach, C. M., Giroud, C., Dorland, W., Hatch, D. R., Barnes, M., Hillesheim, J. C., Aiba, N., Ball, J., Ivanov, P. G. & contributors, JET 2020 Toroidal and slab ETG instability dominance in the linear spectrum of JET-ILW pedestals. *Nucl. Fusion* **60**, 126045.

Parisi, J. F., Parra, F. I., Roach, C. M., Hardman, M. R., Schekochihin, A. A., Abel, I. G., Aiba, N., Ball, J., Barnes, M., Chapman-Oplopoiou, B., Dickinson, D., Dorland, W., Giroud, C., Hatch, D. R., Hillesheim, J. C., Ruiz Ruiz, J., Saarelma, S., St-Onge, D. & Contributors, JET 2022 Three-dimensional inhomogeneity of electron-temperature-gradient turbulence in the edge of tokamak plasmas. *Nucl. Fusion* **62**, 086045.

Roberg-Clark, G. T., Plunk, G. G. & Xanthopoulos, P. 2022 Coarse-grained gyrokinetics for the critical ion temperature gradient in stellarators. *Phys. Rev. Res.* **4**, L032028.

Rogers, B. N., Dorland, W. & Kotschenreuther, M. 2000 Generation and stability of zonal flows in ion-temperature-gradient mode turbulence. *Phys. Rev. Lett.* **85**, 5336.